Eur. Phys. J. Special Topics **205**, 27-52 (2012)

DOI: 10.1140/epjst/e2012-01560-0

THE EUROPEAN PHYSICAL JOURNAL SPECIAL TOPICS

Regular Article

Modeling of super-extreme events: An application to the hierarchical Weierstrass-Mandelbrot Continuous-time Random Walk

T.R. Werner[1], T. Gubiec[2], R. Kutner[2], and D. Sornette[3]

[1] Institute of Theoretical Physics, Faculty of Physics, University of Warsaw, Hoża 69, 00681 Warsaw, Poland
[2] Institute of Experimental Physics, Faculty of Physics, University of Warsaw, Hoża 69, 00681 Warsaw, Poland
[3] ETH-Zürich, Department of Management, Technology and Economics, Kreuzplaz 5, 8032 Zürich, Switzerland

Received 23 November 2011 / Received in final form 09 March 2012
Published online 01 May 2012

Abstract. We analytically demonstrate and numerically simulate two utmost cases of dragon-kings' impact on the (unnormalized) velocity autocorrelation function (VACF) of a complex time series generated by stochastic random walker. The first type of dragon-kings corresponds to a sustained drift whose duration time is much longer than that of any other event. The second type of dragon-kings takes the form of an abrupt shock whose amplitude velocity is much larger than those corresponding to any other event. The stochastic process in which the dragon-kings occur corresponds to an enhanced diffusion generated within the hierarchical Weierstrass-Mandelbrot Continuous-time Random Walk (WM-CTRW) formalism. Our analytical formulae enable a detailed study of the impact of the two super-extreme events on the VACF calculated for a given random walk realization on the form of upward deviations from the background power law decay present in the absence of dragon-kings. This allows us to provide a unambiguous distinction between the super-extreme dragon-kings and 'normal' extreme "black swans". The results illustrate diagnostic that could be useful for the analysis of extreme and super-extreme events in real empirical time series.

1 Introduction

One of the most remarkable observation emerging within the natural and socio-economical sciences is that the empirical data which they provide are frequently punctuated by rare extreme events or *black swans*, which can play a dominant role. This observation is usually quantified by power-laws or heavy-tailed probability distributions of event sizes (cf. [1–13] and references therein). However, as it was pointed out in [13], there is empirical evidence that some important events beyond power laws

do exist. In this context, the concept of *super-extreme events*, *outliers* or *dragon-kings* was introduced there.

By the super-extreme event, outlier or dragon-king[1] we mean an event with size or characteristics that are abnormally different from those of other events in a random sample taken from a given population [15]. The dragon-king is an anomaly, and it is usually removed in order to obtain reliable statistical estimations. The term "outlier" emphasizes the fact that such events are often considered to be spurious, leading to discard them as being errors or misleading measurements. In contrast, the term "dragon-king" emphasizes their relevance in the dynamics and the importance of keeping them to be able to understand the generating process. The super-extreme events are statistically complementary to extreme events and can appear sometimes unexpectedly. However, the alternative idea that dragon-kings are often associated with the occurrence of a catastrophe, a phase transition, a bifurcation, or what can be called a tipping point, whose emergent organization produces visible precursors, was also developed in [13].

The main goal of the present work is to analytically demonstrate and numerically simulate two utmost cases of dragon-kings' impact on the (unnormalized) velocity autocorrelation function[2] (VACF) of a stochastic process generated by a random walker. The estimators of the VACF for these cases are derived in a closed analytical form. These formulae are applied to the enhanced diffusion trajectories generated by the hierarchical Weierstrass-Mandelbrot Continuous-time Random Walk (WM-CTRW) studied in [17–19]. This model is a hierarchical version of the canonical Continuous-time Random Walk (CTRW) model [23–25], obtained from the later by introducing a hierarchical spatio-temporal waiting-time distribution (WTD) (cf. Sect. 3.1 in this work as well as Eq. (20) in [18]).

The WM-CTRW formalism is quite generic and flexible as it is able to cover (only by changing its driving parameters) various types of diffusion, ranging from normal diffusion (Brownian motion), to enhanced diffusion[3], ballistic motion, and to Lévy walks. Extreme events are naturally characterized by the spatio-temporal structure of the time series (herein by stochastic simulation) generated by the WM-CTRW model. This structure is explained in details in Sect. 2. The extreme events moderate the relaxation of the system to equilibrium (or partial equilibrium), e.g., by changing this relaxation from an exponential to a power-law form. Our study of the WM-CTRW formalism is partially motivated by the observations that the hierarchical WTD described quite well its empirical counterparts obtained for continuous quotations of the exchange rates on currency exchange markets as well as for share prices trading on stock exchanges.

The present paper is organized as follows. In Sect. 2, the problem is defined along with the definitions of the most relevant quantities used in our study. In Sect. 3, the WM-CTRW formalism is presented and the enhanced diffusion phase is discussed. Section 4 presents the derivation of the VACF including a dragon-king event. The comparison of the predictions of our theoretical formulae for the VACF with the results of the numerical simulations is given in Sect. 5. Finally, Sect. 6 contains our

[1] The poetic term "dragon-king" stresses that (i) we deal with an exceptional event which is a completely different "animal" compared to the usual events, (ii) this event is important, being outside of the power law, like an absolute monarchy standing above the law or as the wealth of a monarch owning a finite part of the whole country, beyond the Pareto distribution of its citizens' wealth [14].

[2] In econometrics this quantity is called "autocovariance".

[3] Enhanced diffusion is a kind of superdiffusion which remains slower asymptotically than ballistic motion.

summary and concluding remarks. The multi-step representation of the propagator is given in Appendix A.

2 Main questions

The principal question addresses in this article is how to recognize a dragon-king among other events within a given time series. We present an explicitly solvable example that allows one to go beyond the intuitive understanding of what can be dragon-kings. Taking the example of general continuous random walks with long-range memory structures, we characterize the following properties that qualify a dragon-king.

(i) The spatial and temporal sizes that define a "sustained dragon-king" or the velocity that defines an "impetuous or shock dragon-king" must be much larger than those of all other events.
(ii) The statistical properties of the time series must be substantially changed when a dragon-king is present, as compared to the 'free case' defined in the absence of such super-extreme event.

Furthermore,

(iii) we assume in this article (as the simplest reference case) that the dragon-king appears unexpectedly, that is, independently of any previous event.

In our simulations as well as analytical calculations, we generate a WM-CTRW time series in which we insert manually either a "sustained dragon-king" or an "impetuous or shock dragon-king" whose size dwarfs any existing structure. Such dragon-kings could be observed "naturally" in WM-CTRW time series only if one would wait long enough. But the size of the introduced dragon-kings is such that this waiting time is extraordinary long, much much larger that the generated time series duration. This gives a first impression about the fact that a super-extreme event can be qualified as being abnormal only with respect to its occurrence frequency compared with those for the rest of the events. In our examples, the dragon-king's appearance can be considered as being caused by some exogenous source.

By using the approach outlined above, we try to somehow imitate a real situation where a dragon-king, e.g., catastrophic volcanic eruption, a huge tsunami wave or the explosion of a nuclear reactor, appeared during the system evolution as an exogenic factor having an unknown and a priori negligibly small occurrence probability. However, the estimated risk associated with this dragon-king (measured by its frequency of occurrence multiplied by an estimated cost of expected losses) can be extremely large. The investigations of stochastic processes punctuated by super-extreme events present a generic theoretical challenge of increasing practical importance.

Our practical goal herein is to answer the question of how much the stationary velocity autocorrelation function, $C(\Delta t)$, characterizing a given time series (or a random walk trajectory), is changed if this time series is suddenly punctuated by a single-step super-extreme event. In the present work, the metrics we use to quantify the impact of dragon-kings are $C(\Delta t)$ together with some waiting-time distributions (WTD).

As mentioned above, we consider two types of super-extreme events:

(i) the long-drawn event of super-extremely long duration time, t_d (cf. Fig. 1) and
(ii) the shock, or sudden jump, X_d, of a random walker displacement X, which has super-extreme velocity, v_d, (cf. Fig. 2).

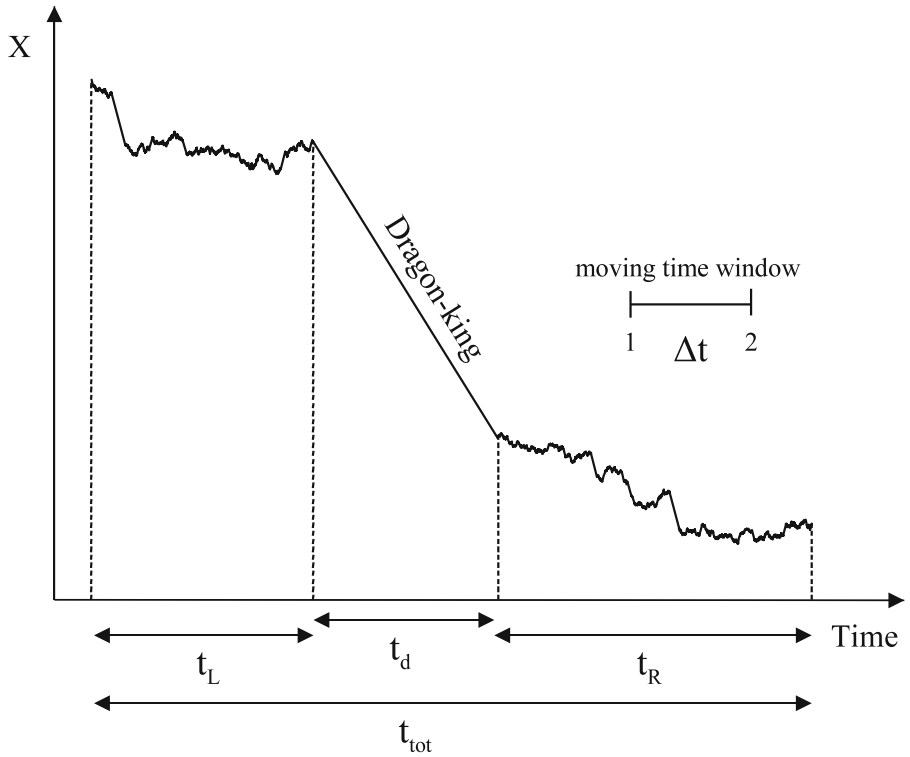

Fig. 1. Schematic time series of a single realization of one-dimensional random walk over a total duration t_{tot} containing the dragon-king (represented by the longest sloping solid straight line) having constant velocity v_d and duration time t_d. The random walk trajectories before and after the occurrence of the dragon-king have duration times t_L and t_R, respectively. Obviously, $t_{tot} = t_L + t_d + t_R$.

The resulting VACF, in the presence of a dragon-king, is denoted below by $C_d(\Delta t)$.

The VACF is defined as the following temporal average

$$\begin{aligned} \mathrm{VACF}(\Delta t) &= \langle v(t')\, v(t'+\Delta t)\rangle - \langle v(t')\rangle \langle v(t'+\Delta t)\rangle \\ &= \langle v_1\, v_2\rangle\,(\Delta t) - \langle v_1\rangle \langle v_2\rangle \\ &= \begin{cases} C(\Delta t), & \text{no dragon-king,} \\ C_d(\Delta t), & \text{with a dragon-king,} \end{cases} \end{aligned} \tag{1}$$

where $\langle \ldots \rangle$ denotes the moving time average within a given time-window $0 \leq t' \leq t_{tot} - \Delta t$ with $\Delta t \leq \Delta t_{max} \ll t_{tot}$, where Δt_{max} is the maximal value of Δt. Here t_{tot} is the total duration time or total time span of a given trajectory (cf. Figs. 1 and 2 where the horizontal time axis corresponds to the variable t'. For further explanations, see Sects. 3 and 4). The velocity of the random walker is $v(t') \stackrel{\text{def.}}{=} [X(t') - X(t' - dt)]/dt$, where the time-discretization step is $dt \leq min(\Delta t, t')$. We denote by v_1 and v_2 the velocities at the beginning and at the end of the time-window of duration Δt.

In order to mimic a real-life situation where we would only have access to a single time series of the realization of a random process, we conider a single random walk trajectory and study its properties in windows of fixed duration Δt running over the whole time series (for further discussion, see Appendix A.). The averaging is performed over this ensemble of time windows of duration Δt. The issues concerning

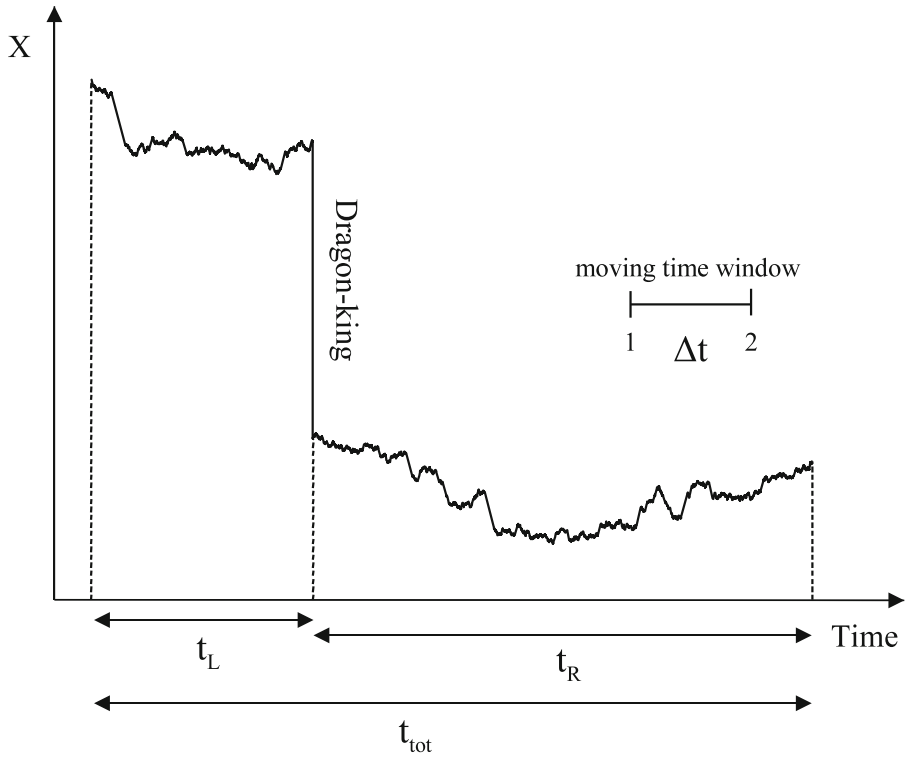

Fig. 2. Schematic time series of a single realization of one-dimensional random walk containing a dragon-king in the form of a shock (represented by the longest vertical solid straight line). The random walk trajectories before and after the dragon-king have duration times t_L and t_R, respectively while the duration time of the shock is $t_d = dt$ being so short that it cannot be visualized in the plot (obviously, $t_{tot} = t_L + dt + t_R$).

ergodicity and its possible breaking have been studied in several articles [20,27–29] (and references therein) in the context of fractional diffusion. In the context of the present implementation of the WM-CTRW model, we consider briefly the property of ergodicity in Sect. 3.

Both quantities $C(\Delta t)$ and $C_d(\Delta t)$ are studied analytically (in Sects. 3 and 4) and numerically simulated (in Sect. 5). Our task is to find relations between $C(\Delta t)$ and $C_d(\Delta t)$ and verify them by simulations for the two dragon-king types (i) and (ii) mentioned above, in the regimes of parameters of the WM-CTRW model that give non-trivial superdiffusion or persistent enhanced diffusion.

3 Outline of the hierarchical Weierstrass-Mandelbrot Continuous-time Random Walk

The task of this section is to outline the hierarchical WM-CTRW formalism most significant elements, which are useful for our analysis and, in particular, for our analysis in the frame of the mentioned above enhanced diffusion phase. This phase is interesting by itself as it combines seemingly opposed very useful properties of the system. That is, it combines superdiffusivity and convergence of the time average. Notably, an explicit form of $C(\Delta t)$ in the absence of a dragon-king was already described in details in our earlier articles [17–19].

3.1 Definition of the WM-CTRW formalism. Single-step quantities

The Weierstrass-Mandelbrot Continuous-time Random Walk is defined by the hierarchical non-separable spatio-temporal waiting-time distribution (WTD). This WTD[4] is given by the following weighted hierarchical series

$$\psi(x,\,\delta t) = \sum_{j=0}^{\infty} w(j)\psi_j(x,\,\delta t), \tag{2}$$

where x is the walker single-step spatial displacement (increment) passed (with constant velocity) within the time interval δt and the weight $w(j)$ is given by the geometric probability distribution

$$w(j) = \frac{1}{N^j}\left(1 - \frac{1}{N}\right), \quad N > 1, \quad j = 0, 1, 2, \ldots, \tag{3}$$

where j is a hierarchy level index. This weight can be interpreted as the occurrence probability of exactly j consecutive successes in some Bernoulli series, where $1/N$ is the probability of a single success; the conditional single-level WTD, $\psi_j(x,\,\delta t)$, is assumed in the factorized form of two different single-variable spatial and temporal border probability distributions $\phi_j(x)$ and $\chi_j(\delta t)$ (based on the scaling functions f and h, respectively)

$$\begin{aligned}\psi_j(x,\,\delta t) &= \phi_j(x) \times \chi_j(\delta t)\\ &= \frac{1}{v_0 v^j \delta t} f\left(\frac{|x|}{v_0 v^j \delta t}\right) \times \frac{1}{\tau_0 \tau^j} h\left(\frac{\delta t}{\tau_0 \tau^j}\right).\end{aligned} \tag{4}$$

In expression (4), we used a simple representation of a random walk (but not random jumps or flights). That is, the assumed spatial and temporal scaling functions have the form

$$f\left(\frac{|x|}{v_0 v^j \delta t}\right) = \frac{1}{2}\,\delta\left(\frac{|x|}{v_0 v^j \delta t} - 1\right) \tag{5}$$

and

$$h\left(\frac{\delta t}{\tau_0 \tau^j}\right) = \exp\left(-\frac{\delta t}{\tau_0 \tau^j}\right), \tag{6}$$

respectively[5]. The mean duration time, $\tau_0 \tau^j\ (\geq 1)$, of the random walker single step and its velocity, $v_0 v^j$, are both associated with the j^{th} level of the spatio-temporal stochastic hierarchy. This level is the same for temporal and spatial border distributions, introducing the spatio-temporal coupling in Definition (2). Indeed, this coupling is responsible for the combination of superdiffusivity and convergence of the time average mentioned at the beginning of this section. Herein, we marked the calibration parameters, i.e., the corresponding units, by τ_0 and v_0.

As it is seen from Definition (2) of the WTD, our WM-CTRW formalism belongs to the *non-separable* category of CTRW, where spatial and temporal variables are

[4] The complete definition of the WM-CTRW model additionally requires a special treatment of the first step of the random walker [18]. However, this treatement is irrelevant when the moving average is calculated, as it is in our case. Therefore, we do not consider explicitly this special treatment in this work.

[5] Obviously, detailed forms of the scaling functions f and h are less important for macroscopic displacement and asymptotic long time, respectively. Here, we used their simple explicit forms to make our calculations easier.

non-separable. The coupling mentined above makes the diffusion phase diagram [17,18] much richer than that for separable category of the CTRW formalism.

From (2), it is easy to derive useful temporal and spatial single-step moments

$$\begin{aligned}\langle \overline{\delta t} \rangle = \overline{\langle \delta t \rangle} &= \int_0^\infty d(\delta t)\, \delta t\, \psi(\delta t) \\ &= \tau_0 \begin{cases} \frac{1-1/N}{1-\tau/N}, & \text{for } \alpha > 1, \\ \infty, & \text{for } \alpha < 1 \end{cases} \end{aligned} \tag{7}$$

where $\alpha \overset{\text{def.}}{=} \ln N / \ln \tau$, the border temporal part of WTD $\psi(\delta t) \overset{\text{def.}}{=} \int_{-\infty}^{\infty} dx\, \psi(x, \delta t)$, and

$$\begin{aligned}\langle \overline{x^2} \rangle = \overline{\langle x^2 \rangle} &= \int_{-\infty}^{\infty} dx\, x^2\, \psi(x) \\ &= (b_0)^2 \begin{cases} 2\,\frac{1-1/N}{1-b^2/N}, & \text{for } \beta > 2, \\ \infty, & \text{for } \beta < 2 \end{cases} \end{aligned} \tag{8}$$

where $b_0 = v_0 \tau_0$, $b = v\tau$, $\beta = \ln N / \ln b$, and border spatial part of the WTD $\psi(x) \overset{\text{def.}}{=} \int_0^\infty d(\delta t)\, \psi(x, \delta t)$. We term parameters α and β the *temporal* and *spatial border exponents*, respectively. They control all phases of diffusion [16–18]. In the subsequent considerations, we study the enhanced diffusion regime defined by $\alpha > 1$ and $\beta < 2$ (further constraints, given by Inequalities (11), are shown in Sect. 3.2). Herein, we do not consider the special marginal cases where $\alpha, \beta = 1, 2, \ldots$, take positive integer values.

In expressions (7) and (8), the notation $\overline{g(x)}$ represents the average of the function $g(x)$ over the spatial variable (herein denoted as x). Note that all averages in Sect. 3 are performed over statistical ensemble. They are thus purely theoretical quantities.

3.2 Remarks concerning the enhanced diffusion regime

The hierarchical WM-CTRW model is defined by the requirement that $\langle \overline{\delta t} \rangle$ is finite [18], which according to (7) is equivalent to the case where $\alpha > 1$. When this holds, the temporal WTD is an asymptotic exponential function characterized by the mean-time $\langle \overline{\delta t} \rangle$ given by the upper expression in (7). Hence, the necessary condition for ergodicity to hold is obeyed in our case, namely

(a) the possibility that the measurement time of the time series, t_{tot}, is sufficiently long compared to the characteristic time scale $\langle \overline{\delta t} \rangle$. Therefore, all averages over time can be performed in this case and
(b) in our stationarized WM-CTRW model, these time averages are independent of the imposed initial condition.

If at least one of these conditions was violated, the ergodicity of the system would be broken. This is also true for the time series containing our dragon-kings.

The question of whether it is possible to exchange with a good approximation an average over an ensemble of trajectories by the corresponding time averages (for a sufficiently long time) over a single trajectory is still a challenge. This is a typical challenge not only for different versions of the CTRW (discussed in several articles [20,27–29]) but also for any empirical time series. For the present work, it would be sufficient to prove ergodicity for the VACF. But even this restricted request remains challenging. To make progress, we will be working in the following within the

conjecture that any sufficiently long realization of the process contains enough statistical information about it so that we can characterize useful differences in the VACF and the WTD functions when dragon-kings are present compared with the situation when they are absent.

According to the canonical CTRW formalism, the WTD given by Eq. (2) is a basic dynamical quantity that is sufficient to construct the propagator of the WM-CTRW model (see Appendix A. for details). In the Fourier-Laplace (k, s) domain, the propagator takes the well-known generic form [24]

$$\begin{aligned}\tilde{P}(k,s) &= \int_0^\infty d(\Delta t) \int_{-\infty}^{\infty} dX P(X,\Delta t) \\ &= \frac{1}{s}\frac{1-\tilde{\psi}(k=0,s)}{1-\tilde{\psi}(k,s)} \ . \end{aligned} \tag{9}$$

The propagator $P(X, \Delta t)$ is defined as the probability density of finding the walker at position X and time Δt under the condition that initially the walker was at the origin. In this notation, the initial condition was, for simplicity, not explicitly specified. Herein, $\tilde{P}$ means the Fourier-Laplace transform of P.

Within the WM-CTRW model, the propagator for enhanced diffusion, that is for the case considered in this work, was derived in the form [16–18]

$$\tilde{P}(k,s) \approx \frac{1}{s}\frac{1}{1+D\,k^2/s^\eta} \tag{10}$$

where the condition of existence of this expression, $D\,k^2/s^\eta \ll 1$, was fulfilled in the derivation. Herein, the so-called *fractional diffusion exponent* η obeys the following inequalities

$$\begin{aligned} 1 < \eta = 1 + 2\alpha\left(\frac{1}{\beta}-\frac{1}{2}\right) < 2 \\ \Leftrightarrow \frac{1}{2} < \frac{1}{\beta} < \frac{1}{2}+\frac{1}{2\alpha} \end{aligned} \tag{11}$$

and, for the so-called *fractional diffusion coefficient*, we obtain the expression

$$D = \frac{1}{\langle\overline{\delta t}\,\rangle}\frac{1-1/N}{\ln N}\pi\alpha\frac{(2-\eta)}{|\sin(\pi\,\eta)|}. \tag{12}$$

This coefficient is finite although the single-step mean-square displacement (8) diverges. This is not too surprising because, most significantly, the time-dependent single-step mean-square displacement, $\overline{x^2(\delta t)} = \int_{-\infty}^{\infty} dx x^2\,\psi(x,\delta t)$, and mean time $\langle\overline{\delta t}\rangle$ are finite (cf. [16] for details). We can state that diffusion is enhanced by the broader distribution of single-step displacements.

An approximate scaling form of the propagator (10) in real space and real time is presented in Appendix B.

Besides, in [17,18], it was proved that the fractional diffusion exponent η drives the asymptotic time dependence of the mean-square displacement of the walker (cf. Eqs. (21) in [17] and (11) in [18]),

$$\overline{X^2(\Delta t)} \approx \frac{2\,D}{\Gamma(\eta+1)}\,(\Delta t)^\eta, \tag{13}$$

where $X(\Delta t)$ is the displacement of the walker found at time Δt (cf. Table 2 and diffusion phase diagram in Fig. 2 in [17] as well as Table 1 and diffusion phase diagram shown in Fig. 1 in [18]).

A significant question of the WM-CTRW formalism is how to relate the displacement X to the single-step displacement x. The answer is typical for the CTRW formalism. The corresponding displacement of the walker is the summation of increments $X(t') = \sum_{j=1}^{n} x_j$, where $\sum_{j=1}^{n}$ denotes the sum over successive steps x_j of the walker forming the segment of the trajectory until the time t' which consists of n steps. Moreover, we have $t' = \sum_{j=1}^{n} \delta t_j$. Note that the number of steps is a quantity that is well defined for each single trajectory taken separately, even if finally we sum over many trajectories when calculating averages (for instance, see Appendix A.).

Note that the times t_L and t_R are defined for each single trajectory or realization of the MW-CTRW and we have the following summation $t_J = \sum_{j=1}^{n_J} \delta t_j$, $J = L, R$. Hence, the total time is given by $t_{tot} = t_L + t_d + t_R$ (cf. Figs. 1 and 2).

Expressions (2)–(6) enable simulating a random walk trajectory (schematically shown in Figs. 1 and 2) in continuous time. This is because they define the corresponding stochastic dynamics (considered in Sect. 5.1).

The WM-CTRW defines a stationary stochastic process valid only for the case where the mean waiting-time, $\langle \delta t \rangle$, is finite, i.e., for the case where the temporal exponent $\alpha > 1$ (cf. Eq. (7) as well as Eqs. (4) and (5) in [18]). Under these conditions, the diffusion exponent $\eta = 2H$, where $1/2 < H < 1$, is the well known Hurst exponent [26]. All our analytical calculations are confined to the case where the mean-square displacement is finite for a finite time and superlinearly increases with time for asymptotically long times. That is, we are confined to the superdiffusion phase where $1 < \eta < 2$ (enhanced diffusion phase). This regime is interesting because dragon-kings could be argued to be least relevant in this phase. Our goal is to demonstrate that dragon-kings make a significant impact even in such a superlinear phase.

For enhanced diffusion, we derived the VACF in the absence of a dragon-king in the form (cf. Eq. (13) in [18])

$$C(\Delta t) = \frac{2\, D_{st}}{\Gamma(\eta - 1)} \frac{1}{\Delta t^{2-\eta}}, \tag{14}$$

where the fractional diffusion coefficient is the quantity $D_{st} = D/(2 - \eta)$ associated with the stationarized random walk [18] (cf. Table 1 in [18]). Then, no initial instant is favoured.

As the fractional diffusion exponent $\eta < 2$, the velocity autocorrelation function, $C(\Delta t)$, given by Expression (14) vanishes for extremely long Δt by following a power law decay. In Sect. 4, we prove that the presence of a dragon-king in the time series leads to violation of this property.

4 Reference formulae for $C_d(\Delta t)$

In this section, we consider useful properties of two different types of reference relations between the estimator of $C_d(\Delta t)$ and the estimator of some VACF, $C(\Delta t)$, concerning a time series in the absence of any dragon-king. That is, in Sect. 4.1, we consider the first type of this relation for the case of sustained dragon-king (case (i) of Sect. 2) while we study in Sect. 4.2 the second type for the case of a shock (case (ii) of Sect. 2).

4.1 $C_d(\Delta t)$ for the case of sustained dragon-king

By assuming that random walks before and after the dragon-king appearance within the time series are statistically identical (although corresponding trajectories could be quite different), we can write, by neglecting unavoidable fluctuations, that in Eq. (C.15) (cf. C.1) the partial velocity autocorrelation functions obey $C_L(\Delta t) = C_R(\Delta t) = C(\Delta t)$. These equalities enable transforming Eq. (C.15) into a stationary form

$$C_d(\Delta t) = \frac{1-\gamma_d - 2\Delta t/t_{tot}}{1-\Delta t/t_{tot}}\, C(\Delta t) + \frac{1}{1-\Delta t/t_{tot}}\left[\gamma_d\left(1-\frac{\gamma_d}{1-\Delta t/t_{tot}}\right) - \frac{\Delta t}{t_{tot}}\right] v_d^2, \tag{15}$$

which is our first reference formula enabling several applications discussed below.

The main difference between $C(\Delta t)$ and $C_d(\Delta t)$ is that the former asymptotically vanishes while the latter does not. This difference provides a tool that allows one to distinguish a power-law relaxation, controlled by rare extremes or black swans, from a decay controlled by the dragon-king. We consider Formula (15) as a reference one, also relevant for more complex cases.

If Assumption (C.18) in C.1 holds, further simplification of Eq. (15) can be made:

$$C_d(\Delta t) \approx (1-\gamma_d)\left[C(\Delta t) + \gamma_d\, v_d^2\right]. \tag{16}$$

This expression depends upon two parameters γ_d and v_d fully characterizing the dragon-king. These parameters can be easily determined, e.g., from the initial and asymptotic nonvanishing values of $C_d(\Delta t)$. Predictions obtained from this simple formula are compared in Sect. 5 with the corresponding simulation results.

4.2 $C_d(\Delta t)$ for the case of a shock

In this section, we consider a dragon-king in the form of a shock (cf. case (ii) of Sect. 2). By analogy with case (i) of a sustained dragon-king, we set in Eq. (C.20) (cf. C.2) $C_L(\Delta t) = C_{LR}(\Delta t) = C_R(\Delta t) = C(\Delta t)$ that, in the case of no drift in the system, simplifies (C.20) into the form

$$C_d(\Delta t) = \frac{t_{tot} - \Delta t - 2dt}{t_{tot} - \Delta t}\, C(\Delta t) + \frac{(v_L + v_R)\, X_d}{t_{tot} - \Delta t} - \left(\frac{X_d}{t_{tot} - \Delta t}\right)^2, \tag{17}$$

where $X_d = dt\, v_d$ is the value of the shock. Note that v_L and v_R are velocities of the walker, which are separated by the time interval $2\Delta t$. By definition of the time step dt, we have $dt \ll t_{tot} - \Delta t$. Hence, Eq. (17) again assumes a simpler form

$$C_d(\Delta t) = C(\Delta t) + \frac{(v_L + v_R)\, X_d}{t_{tot} - \Delta t} - \left(\frac{X_d}{t_{tot} - \Delta t}\right)^2, \tag{18}$$

which is our second reference formula (the first one is given by Eq. (15)). This formula is further modified in Sect. 5 to make $C_d(\Delta t)$ better suited for comparison with our results obtained by simulations.

5 Algorithm and results

5.1 Stochastic dynamics

The stochastic dynamics algorithm simulating successive single-step displacements of the walker following the WM-CTRW model consists of three stages, as follows.

(i) The drawing of the hierarchy level index j from distribution (3) in each spatio-temporal step separately.
(ii) The calculation of the duration time δt of the single step (or its elapsed time) from the stochastic equation

$$\delta t = -\tau_0 \tau^j \ln(1 - R), \tag{19}$$

which simulates an exponential distribution of inter-event times (6), where $R \in [0, 1[$ is a random number drawn from the random number generator (or from the uniform distribution confined to a unit interval). Note that Eq. (19) is equivalent to Eq. (6) (after application of the well known method of inversion of the cumulative distribution function).
(iii) The determination of the single-step displacement using the equation

$$x(\delta t) = \xi \, v_0 \, v^j \delta t, \tag{20}$$

where stochastic variable ξ is a dichotomic noise (i.e., $\xi = +1$ or -1 with equal probability 1/2) and $x(\delta t) \stackrel{\text{def.}}{=} X(t') - X(t' - \delta t)$, where t' is the current time (and not a time interval).

In this way, the construction of a single time-continuous trajectory of a random walk is possible. Obviously, the parameters τ_0, τ, v_0, and v were fixed at the beginning of the whole simulation. Further in the text and in all our simulations, we set the parameters $\tau_0 = 1$ and $v_0 = 1$.

In fact, the above-mentioned trajectory is constructed in the frame of a version of the CTRW that is not made stationary, i.e., for which there is no special treatment of the initial step [17,18,24]. In this version, the hierarchical spatio-temporal waiting-time distribution (2) for the initial step is the same as that for all other steps. This equality of distributions is possible because in simulations we deal with moving-averages, which by definition, average over the initial state, thus supplying the required asymptotic stationary VACF. Indeed, we compare this VACF with the corresponding VACF obtained theoretically within the WM-CTRW model. One should keep in mind that the version of the CTRW that is made stationary is such that it treats differently the waiting-time distribution for the initial step within the WM-CTRW formalism[6] [18].

The above given algorithm was used in Sect. 5.2 to simulate the required basic random-walk trajectory. The trajectory constructed in this way is punctuated "manually" by the sustained dragon-king or by the shock dragon-king. Preparation of the former dragon-king requires some explanation.

5.1.1 Preparation of the sustained dragon-king

The stochastic dynamics defined by Eqs. (19) and (20) is controlled by three random variables j, R, and ξ. Only two of these three variables are responsible for the size of a single step: (a) the hierarchy level index j, drawn from the distribution (3), and (b) the random number R. For the case of the sustained dragon-king, this dynamics

[6] It can be proved that the WM-CTRW formalism, even asymptotically, is more general than the fractional Brownian motion introduced by Mandelbrot and van Ness [26]. This is because the propagator derived within the WM-CTRW formalism can be non-Gaussian (cf. Appendix B).

is simplified by replacing Eq. (19) by the corresponding simplified expression[7]

$$\delta t = t_d = \tau_0 \tau^{j_d}. \tag{21}$$

The size of the sustained super-extreme event is controlled solely by a single random variable $j = j_d$ as is the velocity of the sustained dragon-king $v_d = v_0\, v^{j_d}$, its duration time $t_d = \tau_0\, \tau^{j_d}$, and displacement $x_d = \xi\, b_0\, b^{j_d}$, where $b_0 = v_0\, \tau_0$ and $b = v\tau$. The stochastic process defined by Eqs. (21) and (20) is simplified because it is discretized in time and space, where

$$x(\delta t) = X_d = \xi v_0 \tau_0 v^{j_d} \tau^{j_d} = \xi b_0 b^{j_d}. \tag{22}$$

As the index j_d of a given dragon-king is fixed, the inter-event time for this process does not fluctuate.

We deal with two stochastic processes: (i) the first one which prepares the WM-CTRW trajectory or stochastic spatio-temporal hierarchy of events and (ii) the second process which generates the sustained dragon-king from the simplified, discrete in space and time hierarchical random walk. In fact, the latter process is also used in Sect. 5.1.2 to illustrate the definition of the black swan.

Therefore, it is easy to separate in simulations the sustained dragon-king from the other events belonging to the stochastic spatio-temporal hierarchy of events (cf. Sect. 5.1.2). Namely, it is sufficient to choose the level index j_d much larger than the maximal level index $j = j_{max}$ of the hierarchy constituting the WM-CTRW model.

5.1.2 Hierarchical random walk and black swans

It is decisive for our considerations that the ratio of successive weights

$$\frac{w(j+1)}{w(j)} = \frac{1}{N}, \tag{23}$$

is already j independent. This means that steps defined by the level index j are N times more likely than those of the next step of the higher order of $j+1$. Therefore, one expects (on the average) that the walker will perform N^j shorter steps before performing the next step of the higher order. Hence, we can explain how extreme events or black swans control the hierarchical spatio-temporal structure of events in the frame of a simplified hierarchical random walk.

Subsequently we consider, as a typical quantity, the mean-square displacement of the simplified, discrete in space and time hierarchical random walk

$$\overline{X^2}(L) = \overline{\left(\sum_{l=1}^{L} x_l \right)^2} = L\overline{x^2}, \tag{24}$$

(where $\overline{g}$ denotes an ensemble average of g, as in Sect. 3.1), L is the total number of random walk steps, x_l is a single-step displacement and $\overline{x^2}$ is its mean-square value. In this derivation, we neglected the off-diagonal term $\sum_{l \neq l'}^{L} \overline{x_l x_{l'}}$ or crossed correlations between successive single-step displacements in comparison with the diagonal term

[7] Instead of a simplified dynamics, defined by Eqs. (21) and (22), we could use the full dynamics defined by Eqs. (19) and (20) with $j = j_d$ and R equal, e.g., to the maximal random number R_{max} drawn during the whole simulation. Fortunately for our simulation, the simplified dynamics produced adequately the sustained dragon-king.

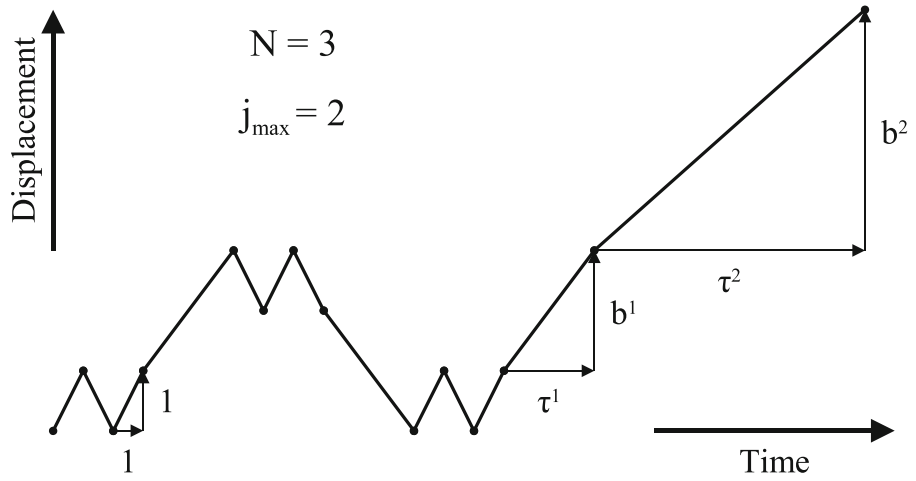

Fig. 3. Schematic trajectory of hierarchically ordered steps (τ^j, b^j) presented, for simplicity, for $N = 3$, $j_{max} = 2$ and calibration parameters $\tau_0 = 1, b_0 = 1$. We assumed $j_{max} \gg 1$ in our calculations. Herein, the extreme event or black swan is defined by the pair of components $(\tau^{j_{max}=2}, b^{j_{max}=2})$ directed by $j_{max} = 2$.

$L\overline{x^2}$. This is justified by the definition of the process, which invokes independent step draws.

In Fig. 3, the schematic illustration of the above considerations is shown by using a part of the trajectory or random walk realization consisting of hierarchically ordered steps $(\tau_0\,\tau^j, b_0\,b^j)$, for $j = 0, 1, 2$. Herein, we neglected (i) fluctuation of the number of hierarchy levels js as well as (ii) their random succession. Thus, we plotted the ordered trajectory within the time-space frame of coordinates. In fact, we made a transformation from the stochastic hierarchy to its deterministic counterpart. The explanation of the concept of black swans becomes now more convenient.

We can easily derive the useful relation between the single-step mean-square displacement, $\langle x^2 \rangle$, which originates from the simulated trajectory and the maximal level, j_{max}, of the hierarchy contained in it. Indeed, the level j_{max} defines the extreme event or black swan by the pair of components $(\delta t_{max} = \tau_0\,\tau^{j_{max}},\ x_{max} = b_0\,b^{j_{max}})$. This quantity, for a large number of steps $L \gg 1$ or $j_{max} \gg 1$, is given by

$$\begin{aligned}\frac{\langle x^2 \rangle}{(b_0)^2} &\approx \frac{N^{j_{max}}}{L}\,(b^2)^0 + \frac{N^{j_{max}-1}}{L}\,(b^2)^1 + \frac{N^{j_{max}-2}}{L}\,(b^2)^2 \\ &\quad + \ldots + \frac{N^0}{L}\,(b^2)^{j_{max}} = \frac{N^{j_{max}}}{L}\,\frac{(b^2/N)^{j_{max}+1} - 1}{b^2/N - 1} \\ &\approx \frac{\overline{x^2}}{(b_0)^2}. \end{aligned} \tag{25}$$

We used here a kind of an ergodic hypothesis, which for this particular considerations seems to be obvious.

By using Eqs. (24) and (25), we proved in Appendix D. that, for $\beta < 2$, the summarized quantity $\overline{X^2}$ is fully determined by a single step of extreme event x^2_{max} (cf. Eq. (D.3)). This result is exactly what is needed for illustration of our considerations. That is, the quantities (herein the mean-square displacement of the process) characterizing the system are mainly expressed by the corresponding quantities (herein, a single-step displacement) defining the black swans.

As expected, for Brownian motions (that is, for the case of $\beta > 2$ in Eqs. (D.1), (D.2) and (D.3)), the factor preceding L in the second formula in (D.2) and (D.3) equals, in fact, the corresponding factor present in formula (8). However, the absence of the factor 2 is here caused by the absence of fluctuations of inter-event times.

Note that, in the case of the WM-CTRW, we obtain results analogous to those presented by Eqs. (D.2) and (D.3). However, their derivation is much more complicated in this case. The threshold property exhibited by these equations is typical of the behavior of other key quantities, like volatilities or correlation functions.

We are now ready to answer the question concerning the distribution of the single-step displacements $|x| = b_0 b^j$ of the walker. This answer is based on the change of variables from j to $|x|$. Hence, the corresponding (normalized) distribution $\tilde{w}(|x|)$ takes the Pareto form

$$\tilde{w}(|x|) \approx \frac{1}{b_0} \frac{\beta}{(|x|/b_0)^{\beta+1}}, \tag{26}$$

where $|x| \geq b_0$. In fact, Eq. (26) holds only for $|x| \gg b_0$. As found in [12,25], the power-law distribution of events leads to the Fréchet distribution of extreme events. For asymptotic values of the argument, this distribution preserves the power law with exponent of $\beta + 1$. Note that Eq. (26) is valid for all values of β. That is, black swans are always present in the system. However, only for $\beta < 2$ their influence dominates, leading to power laws.

To conclude this discussion, we can say that square of the linear size of the walk (herein, the mean-square displacement) is controlled by extreme events or black swans if this square scales with the number of steps according to some power-law, i.e., if the walk is a certain type of fractional random walks. Otherwise, Brownian motions dominate without influence of black swans (although they are present in the system). In this way, the threshold value 2 of exponent β is a discriminator of black swans' activity.

We can now identify an event as a sustained dragon-king if the j_d index of this event distinctly exceeds that of j_{max}, i.e., when we have at least that $j_d \geq j_{max} + 2$. Note that the result of simulations for $j_d \geq j_{max} + 1$ agrees well with the theoretical prediction (cf. plot in Fig. 4 for the curve marked by $j_d = j_{max}(= 12) + 1 = 13$ and Table 1).

5.2 Comparison of theoretical predictions with simulations

We restrict our simulations to an important example of enhanced diffusion defined by $1/\beta$ only slightly smaller than $1/\alpha$. Note that inequality $1/\beta < 1/\alpha$, is equivalent to $v < 1$, i.e., it corresponds to the case where the velocity of the walker for the higher hierarchy level is smaller. In this case, each moment of the arbitrary non-negative order of the (multi-step) displacement is finite at finite times [18,19]. This choice of moments arises from empirical evidences that these moments are always finite. Other choices, concerning other diffusion phases, would also be worth studying. The dragon-king is located "manually" inside the simulated time series in such a way that inequality $\Delta t_{max} \ll t_L, t_R$ is obeyed.

5.2.1 Simulation results for the sustained dragon-king

We now discuss the case where the multiplicative factor preceding v_d^2 in Eq. (15) is positive, which is easy to fulfil. This corresponds to considering inequality $\frac{\Delta t}{t_{tot}} < \gamma_d(1 - \frac{\gamma_d}{1-\Delta t/t_{tot}})$. This inequality is only slightly stronger than $\frac{\Delta t}{t_d} < 1$, yet it is needed for the derivation for $C_d(\Delta t)$ if the sustained dragon-king appears.

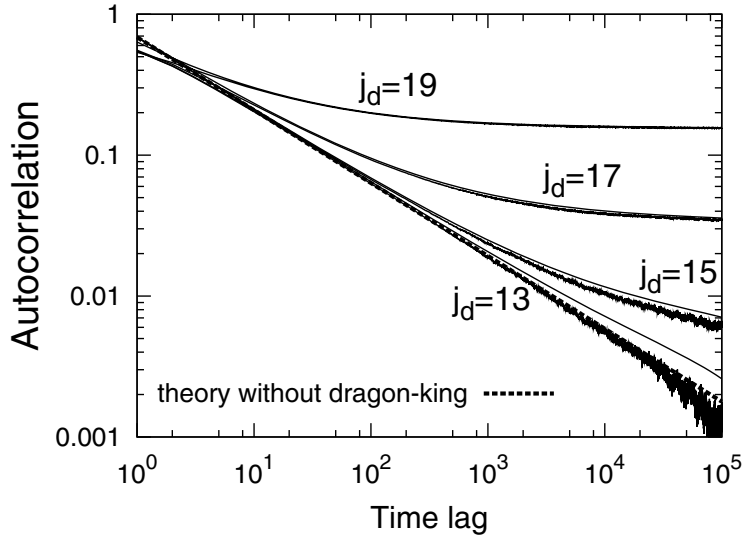

Fig. 4. Comparison of the prediction of Eq. (15) (solid thin curves) with results of simulations (dispersed solid thick curves) for four different values of $t_d/\Delta t_{max} = 1.653, 10.496, 66.651$, and 423.263 which correspond to $j_d = 13$, 15, 17 and 19, respectively. The dashed curve represents the prediction of Eq. (14), i.e., the prediction for the time series in the absence of a dragon-king. All curves were calculated for the same values of $\tau = 2.52, v = 0.992$, and $N = 4$. Notably, theoretical predictions for $j_d = 17$ and 19 are almost indistinguishable (within the resolution of the plot) from results of the corresponding simulations for the whole range of time lag Δt. The presence of the sustained dragon-king twists upward the curve deviating it from the straight line (in the log – log plot).

In Table 1, we present data (in a form of four inverted pyramids of numbers), which define unnormalized statistics, $S(j)$, of the hierarchy levels j's (cf. Sect. 5.1). These data were obtained for fixed common parameters $\tau_0 = 1.0, \tau = 2.520, v_0 = 1.0, v = 0.992$, and $N = 4$. They were used to prepare four trajectories within the WM-CTRW formalism in the presence of sustained dragon-kings. For instance, the row numbered by level $j = 3$ gives, at the intersection with the second column, the number which says how many times (herein, 809231 times) this level appeared in the first trajectory. This trajectory contains the only sustained dragon-king defined by index $j_d = 13$. This index is shown in Table 1 by the bold number 1, at the intersection of row numbered by level $j = 13$ with the second column, again. The successive columns from column three to five contain analogous unnormalized statistics but for higher j_d values[8], i.e., $j_d = 15, 17$, and 19, that is, for stronger sustained dragon-kings. The common bottom of all hierarchies (represented in Table 1 by inverted pyramides of numbers) is placed at the level $j = j_{max} = 12$, that is above any $13 \leq j = j_d \leq 19$.

All sustained dragon-kings are marked in Table 1 by the bold number 1. They are placed in the second through fifth column at intersections with the corresponding rows indexed by levels from $j = j_d = 13$ to $j = j_d = 19$. That is, these levels systematically move away from the common bottom of hierarchies.

Importantly, the left part of the trajectory (preceding the dragon-king appearance) is common for all dragon-kings. The right border of this part is fixed defining the beginning of a dragon-king. Because the total duration time, t_{tot}, of all trajectories is the same, the duration time, t_R, of the part of trajectory placed on the right-hand side of the dragon-king decreases as the duration time t_d increases (i.e., when the index

[8] Eqs. (21) and (22) precisely define the role of index j_d used here.

Table 1. Four unnormalized statistics $S(j)$ of hierarchy levels j's obtained for four sustained dragon-kings.

Level j	$S(j)$ for $j_d = 13$	$S(j)$ for $j_d = 15$	$S(j)$ for $j_d = 17$	$S(j)$ for $j_d = 19$
0	51763445	51439530	49410801	36182538
1	12948042	12866869	12360063	9049915
2	3234819	3214452	3087567	2260332
3	809231	804047	772246	565401
4	202591	201289	193303	141499
5	50583	50521	48326	35374
6	12773	12704	12211	8895
7	3162	3141	3012	2212
8	811	801	765	565
9	192	191	181	128
10	48	47	43	29
11	6	6	6	4
12	5	5	4	3
13	**1**	0	0	0
14	0	0	0	0
15	0	**1**	0	0
16	0	0	0	0
17	0	0	**1**	0
18	0	0	0	0
19	0	0	0	**1**

j_d increases). Therefore, the statistics $S(j)$ of hierarchy levels j's, shown in Table 1, decreases as the level defining the sustained dragon-king, j_d, is rised (because then the corresponding trajectory or time series, placed on the right-hand side of the dragon-king, is shorter). Therefore, for example, the number 128 placed at the intersection of the fifth column and the row denoted by the index level $j = 9$ is distinctly smaller than the number 192 placed at the same row but at the intersection with the second column. We hope that Table 1 well illustrates the hierarchical structure of any (long) trajectory simulated within the WM-CTRW formalism. Moreover, the corresponding localisations of the sustained dragon-kings in the space of hierarchy levels relative to the inverted pyramids are also well delineated.

In Fig. 4, we compare the prediction of Formula (15) (thin solid curves) with the results of simulations (dispersed thick solid curves) for four different values of t_d, namely, $t_d/\Delta t_{max} = 1.653$, 10.496, 66.651, and 423.263, which correspond to $j_d = 13$, 15, 17, and 19, respectively. Note that the current width of the time window, Δt, (called also *time lag*) ranges from $\Delta t = dt$ up to $\Delta t = \Delta t_{max} = 10^5\, dt$ with the time step, $dt = 1$, while $t_{tot} = 1400\, \Delta t_{max}$ is the same for all statistics $S(j)$ shown in Table 1. In fact, the predictions of both Formulae (15) and (16) cannot be distinguished within the resolution of the figure. The sustained dragon-kings' time lags were calculated for the same value of $\tau = 2.520$ and the single-step displacements were calculated for the common $b = v\,\tau = 2.50$ (where $b_0 = v_0\tau_0 = 1.0$).

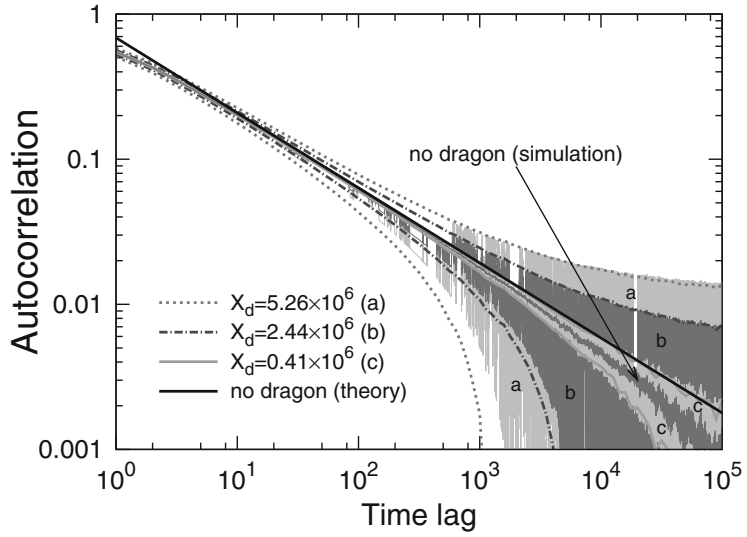

Fig. 5. Comparison of the prediction of Formula (27) (dotted and dashed-dotted curves as well as grey solid one) with results of simulations (corresponding regions having different greyness, additionally marked by a, b and c) for three different values of $X_d = 5.26$, 2.44, and 0.41 [$\times 10^6$]. The black solid curve shows the prediction of Formula (14), i.e., the prediction for the time series simulated in the absence of a shock dragon-king; the corresponding simulated VACF is given for this time series by the innermost (dark) region. All curves were obtained for values of $\tau = 2.52, v = 0.992$, and $N = 4$, which are the same as for the case of the sustained dragon-king.

The upward convexity of the curves in Fig. 4 is due to the presence of the corresponding sustained dragon-king. As expected, the agreement, shown in Fig. 4 between the prediction of Formula (15) and data obtained from simulations, becomes better the further the dragon-king is located from the top of the hierarchy (see the location of the bold number 1 in Table 1). The best agreement is obtained for the largest $j_d = 19$. In other words, the dragon-kings defined by j_d smaller than 19 only slightly positively deviate their corresponding velocity autocorrelation functions, $C_d(\Delta t)$, from their simulational counterparts.

The quantity $C(\Delta t)$, controlled by black swans and given by expression (14), is also plotted in Fig. 4 (the dashed curve) as a reference VACF. In other words, this VACF was calculated for the absence of a dragon-king.

5.2.2 Simulation results for the shock dragon-king

In Fig. 5, we present the results of simulations of the VACF for three different values of the shock size $X_d = 0.41, 2.44$, and 5.26 [$\times 10^6$], which corresponds to $X_d/x_{max} = 1.90$, 11.3, and 24.4, respectively, where x_{max} is the maximal spatial value of the random walk's single step belonging to the simulated hierarchical WM-CTRW trajectory in the absence of a dragon-king. Remarkably, all these shocks are fully exogenous as they were taken from outside of the spatio-temporal structure of time series or random walks. The simulated trajectories have also the total duration $t_{tot} = 1400\,\Delta t_{max}$ and, except for the presence of the dragon-king, all trajectories are identical.

A striking property of simulated VACF's is their dispersion behaving like a certain instability. Therefore, it is more convenient to use a formula that only describes the

dispersion of the data. In principle, this formula could be obtained by replacing the sum of velocities $v_L + v_R$ in Formula (18) by its dispersion $\sigma = \sqrt{\langle (v_L + v_R)^2 \rangle} = \sqrt{2}\sqrt{\sigma_v^2 + C(2\Delta t)}$, where $\sigma_v^2 = \langle v_L^2 \rangle = \langle v_R^2 \rangle$. This replacement is allowed because we assumed, for simplicity, that a shock does not change the type of the random walk.

Moreover, our approach allows us to study a more realistic case, e.g., that in which dispersion is lower than σ defined above. Hence, we propose a more flexible stationary formula

$$C_d(\Delta t) \approx C(\Delta t) \pm \sqrt{2}\,\sigma_f \frac{X_d}{t_{tot} - \Delta t} - \left(\frac{X_d}{t_{tot} - \Delta t} \right)^2, \tag{27}$$

where $\sigma_f \overset{\text{def.}}{=} \sqrt{f\sigma_v^2 + C(2\Delta t)}$ and the phenomenological factor or weight, $0 < f \leq 1$, is the same for all trajectories. As is apparent, we transformed the non-stationary expression (18) to a more useful stationary Expression (27) valid also for the case of the shock dragon-king.

Comparison of the prediction of Eq. (27) with the data obtained by simulations is shown in Fig. 5. In this figure, only small deviations are seen for the choice of the factor $f = 0.30$. The data scatter is reasonably small but it increases with the increase of the ratio X_d/t_{tot}. The origin of this scatter comes from fluctuations of the simulated trajectory, unfortunately resulting also in a spontaneous artificial trend (e.g., as a deviation from the power law in the absence of the dragon-king). Additionally, this trend can be supported by the finite size of the simulated time series.

Note that further simplification of Eq. (27) is also possible

$$C_d(\Delta t) = C(\Delta t) \pm \sqrt{2}\,\sigma_f \frac{X_d}{t_{tot}} - \left(\frac{X_d}{t_{tot}} \right)^2, \tag{28}$$

if the strong but reasonable inequality $\Delta t_{max}/t_{tot} \ll 1$ is obeyed.

6 Summary and concluding remarks

In the present work, we introduced the definitions of two kinds of super-extreme events, the sustained and shock dragon-kings. They were defined specifically in the frame of the hierarchical Weierstrass-Mandelbrot Continuous-time Random Walk.

Furthermore, we discussed the following issues.

(i) We considered the impact of the two distinct types of dragon-kings on the (unnormalized) velocity autocorrelation function.

(ii) By simulations and theoretical analysis, we found that the dragon-king influence decisively changes the original VACF, as determined within the hierarchical Weierstrass-Mandelbrot Continuous-time Random Walk formalism for a wide range of time intervals. The impact of both types of dragon-kings is well pronounced but quite different (cf. the corresponding plots shown in Figs. 4 and 5). Remarkably, the results obtained by simulations agree well with the corresponding predictions of our simple theoretical Formulas (15) and (27) (see again Figs. 4 and 5).

(iii) Furthermore, several intermediate formulas, e.g. (C.13), (C.15), or (C.20), derived for $C_d(\Delta t)$ in this work, can be applied to more complex cases where, for instance, (a) the random walk is changed after the dragon-king appearance, (b) the random walk with drift is considered and (c) dragon-kings cluster in the system.

As it is apparent from Fig. 4, the presence of the sustained dragon-king throws the system away from the state controlled by black swans. The 'fingerprint' of this dragon-king is significant because it convexly twists upward the curve of the autocorrelation dependence on the time lag and distinctly deviates it positively from the power law generated by black swans (cf. Sect. 5.1.2 for details). This deviation is one of the main features distinguishing $C_d(\Delta t)$ from the usual $C(\Delta t)$. This difference allows one to distinguish a power-law relaxation, controlled by black swans, from the decay controlled by the sustained dragon-king. Moreover, this difference can be so distinct that it can effectively be applied as a quantitative tool to detect the sustained dragon-king in an empirical time series.

Moreover, the shock dragon-king also significantly changes $C(\Delta t)$ (Fig. 5). However, this change is different than the change caused by the sustained dragon-king. This change is also well seen by direct comparison of Formulas (15) and (27). Noticeably, the scatter of the data shown in Fig. 5 indicates some instability of the system after the appearance of the shock dragon-king. Indeed, if the empirical VACF reveals such an instability then we can anticipate that the corresponding empirical time series contains the shock dragon-king. In other words, such an anomalous VACF indicates the presence of shocks.

Notably, our considerations proved that sustained and shock dragon-kings can appear in systems characterized by some power law distributions. These distributions seem to be ubiquitous statistical features of natural and socio-economic systems (cf. [1,13,30] and references therein). Indeed, we expect that events defined as the dragon-king events, which can appear there, substantially change the shape of these distributions. That is, the dragon-king events destroy their stability. For instance, in [1], a series of characteristic figures illustrating the occurrence of the power law tails was shown together with corresponding dragon-king events. Both these power law tails and dragon-kings are relevant to various phenomena appearing in very different areas. Besides finance, particularly promising cases for applications of our approach seem to be:

(a) turbulence, where super-extreme events were observed to appear in the distribution of the turbulent velocity fluctuations,
(b) mechanics of rupture, where global failure is considered as a super-extreme event within the material failure process,
(c) neurobiology, where super-extreme events in the distributions of epileptic seizures associated with the strong coupling synchronized regime are observed, and
(d) urbanization where, e.g., the size of Paris can be considered as a dragon-king among all French cities.

In fact, our approach is potentially relevant to the analysis of arbitrary, prolonged time series where the dragon-king can play the role of a fingerprint of possible phase transition or crash precursor (in the case of financial markets for instance).

We thank Armin Bunde for stimulating discussion. This work was partially supported by the Grant No. 119 awarded to the first three coauthors within the First Competition of the Committee of Economic Research, organized by the National Bank of Poland.

Appendix A. Multi-step representation of the propagator

The waiting-time distribution considered herein is the quantity relevant to construct the propagator for the WM-CTRW model. The starting point is a multi-step expansion where the propagator $P(X, \Delta t)$, presented in expression (9), consists of the

unrestricted superposition of the n-step ones, $P(X, \Delta t; n)$,

$$P(X, \Delta t) = \sum_{n=0}^{\infty} P(X, \Delta t; n) \tag{A.1}$$

defined as the probability density to find a walker at position X at time Δt within n steps. Obviously, all propagators take into account (as an initial condition) the fact that the time origin can be chosen arbitrarily in the stationary situation. In order to incorporate this possibility, the first transition of the walker needs a special treatment (for details see [17] as, for simplicity, we do not consider this subtle point in the present article).

For the determination of all n-step propagators, we introduce an auxiliary sojourn probability $\Psi(x, \Delta t)$ that the walker needs at least time Δt to pass the displacement x within a single step. This probability relates to the WTD by the following equality

$$\Psi(x, \Delta t) = \int_{\Delta t}^{\infty} d(\Delta t')\, \psi(x, \Delta t'). \tag{A.2}$$

The multi-step propagators can be now expressed by the following spatio-temporal convolutions

$$\begin{aligned}
&P(X, \Delta t;\ n = 0) = \Psi(X, \Delta t),\\
&P(X, \Delta t; n) = \int_0^{\Delta t} dt_n \int_0^{t_n} dt_{n-1} \ldots \int_0^{t_3} dt_2 \int_0^{t_2} dt_1\\
&\times \int_{-\infty}^{\infty} dX_n \int_{-\infty}^{\infty} dX_{n-1} \ldots \int_{-\infty}^{\infty} dX_2 \int_{-\infty}^{\infty} dX_1\\
&\psi(X_1, t_1)\psi(X_2 - X_1, t_2 - t_1) \ldots\\
&\psi(X_n - X_{n-1}, t_n - t_{n-1})\, \Psi(X - X_n, \Delta t - t_n),\\
&n = 1, 2, 3, \ldots .
\end{aligned} \tag{A.3}$$

Herein, (X_j, t_j), $j = 1, 2, \ldots, n$, denote turning points of the random walk trajectory, where random time instants t_j are located inside the time window Δt. This time window plays the role of a parameter (and not stochastic variable). As is apparent, the n-step propagator is, for $n \geq 1$, the n-fold convolution. That is, for the n-step propagator, the walker completes exactly n single steps while the next (final) one is just under way (generally being not finished). Hence, after Fourier and Laplace transformations, the convolutions transform in geometric series that finally lead to expression (9).

This shows a useful role for the expansion containing the successive steps of the walker (cf. expansion (A.1)). The components of this expansion provides the possibility of a more microscopic insight into the structure of the continuous-time random walk. For instance, this is significant for the simulation of the random walk trajectories where usually an intermediate stage of the procedure explicitly involves some random (but well defined) number of successive steps of the walker.

Appendix B. Approximate expression of the propagator

An approximate form of the propagator (10) expressed in real space and real time was derived in Refs. [21,22] in the following scaling form [16]

$$P(X, \Delta t) = \bar{C}\, \Delta t^{-\eta/2} F(\xi). \tag{B.4}$$

This derivation is based upon the steepest descent method for the scaling variable $\xi = X^2/\Delta t^{\eta} \gg D$. The scaling function is

$$F(\xi) = \xi^{-\bar{\nu}/2} \exp\left(-\frac{\xi^{\nu}}{4\bar{D}}\right). \tag{B.5}$$

The auxiliary exponents are given by

$$\nu = \frac{1}{2-\eta}, \quad \bar{\nu} = \nu - 1, \tag{B.6}$$

and the coefficients are defined by

$$\begin{aligned} \bar{C} &= \frac{1}{2}\left(\frac{\nu}{\pi D}\right)^{1/2} \left(\frac{2D^{1/2}}{\eta}\right)^{\bar{\nu}}, \\ \bar{D} &= \left(\frac{D}{\eta^2}\right)^{\nu} \eta\nu. \end{aligned} \tag{B.7}$$

As it is seen from Eq. (B.4), the fractional dependence of the mean-square displacement of the walker (13), i.e., $\overline{X^2(\Delta t)}$ vs. $(\Delta t)^{\eta}$, can be easily reproduced.

Appendix C. Derivation of formulas for $C_d(\Delta t)$

In this section we derive two different types of relation between the estimator of $C_d(\Delta t)$ and the estimator of some VACF, $C(\Delta t)$, concerning a time series in the absence of any dragon-king. That is, in Sect. C.1, we consider the first relation for the case (i) and the second relation for the case (ii) in Sect. C.2, where both cases were already defined in Sect. 2.

C.1. $C_d(\Delta t)$ for the case of sustained dragon-king (case (i) of Sect. 2)

In this section, we assume that

(a) $dt \leq \Delta t \leq \Delta t_{max} \ll t_L$, t_R and

(b) $\Delta t_{max} \leq t_d$, where Δt_{max} is the maximal value of Δt.

Importantly, assumption (b) is violated for case (ii) defined in Sect. 2. This case is considered below in Sect. C.2.

We divide the expected value of the product of velocities, $\langle v_1 v_2 \rangle(\Delta t)$ in Formula (1) into five weighted different components. They are estimated by the following terms

$$\langle v_1 v_2 \rangle(\Delta t) = \sum_{m=1}^{M=5} \langle v_1 v_2 \rangle_m(\Delta t)\, w_m. \tag{C.7}$$

It is straightforward to derive each component $\langle v_1 v_2 \rangle_m(\Delta t)$ separately by using the proper moving-average estimator. The corresponding weight w_m is readily obtained.

(1) The first component (for $m = 1$) is defined for the case, where both velocities v_1 and v_2 are placed before the dragon-king position. This component together with the corresponding weight are as follows

$$\langle v_1 v_2 \rangle_1(\Delta t) \stackrel{\text{def.}}{=} \frac{1}{t_L - \Delta t} \sum_{t'=dt}^{t_L - \Delta t} v(t')\, v(t' + \Delta t),$$

$$w_1 \stackrel{\text{def.}}{=} \frac{t_L - \Delta t}{t_{tot} - \Delta t} \tag{C.8}$$

and relates to a random walk in the absence of any dragon-king. More precisely, this component represents the situation where velocity v_1 is placed inside the time interval $[0, t_L - \Delta t]$ while the velocity v_2 can be placed both inside this interval or at its right border $t_L - \Delta t$.

(2) For the second component ($m = 2$), velocity v_1 is placed before the position of the dragon-king while velocity v_2 equals the velocity of the dragon-king v_d. The second component and the corresponding weight takes the form

$$\langle v_1 v_2 \rangle_2(\Delta t) \stackrel{\text{def.}}{=} \frac{1}{\Delta t} \sum_{t'=t_L - \Delta t + dt}^{t_L} v(t')\, v_d = \langle v \rangle_L v_d,$$

$$w_2 \stackrel{\text{def.}}{=} \frac{\Delta t}{t_{tot} - \Delta t}, \tag{C.9}$$

where v_d is the velocity of the dragon-king (or the slope of the longest straight line shown in Fig. 1). This term describes the first cross situation where velocity v_1 is located inside the time interval $[t_L - \Delta t, t_L]$ or at its right border while velocity v_2 is placed inside the time-interval $[t_L, t_L + \Delta t]$ or at its right border. We denote by v_d the constant velocity of the dragon-king.

(3) This case is particularly simple as both velocities v_1 and v_2 are equal to v_d. The third component ($m = 3$) is the simplest one and together with the corresponding weight assume the forms

$$\langle v_1 v_2 \rangle_3(\Delta t) \stackrel{\text{def.}}{=} v_d^2,$$

$$w_3 \stackrel{\text{def.}}{=} \frac{t_d - \Delta t}{t_{tot} - \Delta t}. \tag{C.10}$$

This corresponds to the case where both velocities v_1 and v_2 are placed inside the dragon-king's time interval $[t_L, t_L + t_d]$ or velocity v_2 can be also located at its right border.

(4) Herein, velocity v_1 equals the dragon-king's velocity v_d while velocity v_2 is placed after the position of the dragon-king. The fourth component ($m = 4$) and the weight are

$$\langle v_1 v_2 \rangle_4(\Delta t) \stackrel{\text{def.}}{=} \frac{1}{\Delta t} \sum_{t'=t_L + t_d - \Delta t + dt}^{t_L + t_d} v_d\, v(t') = v_d \langle v \rangle_R,$$

$$w_4 \stackrel{\text{def.}}{=} \frac{\Delta t}{t_{tot} - \Delta t} \tag{C.11}$$

corresponding to the second cross case. Precisely, velocity v_1 is placed inside the dragon-king time interval $[t_L + t_d - \Delta t, t_L + t_d]$ for this case or at its right border while velocity v_2 is placed inside the time interval $[t_L + t_d, t_L + t_d + \Delta t]$ or at its right border.

(5) For the fifth component ($m = 5$), positions of both velocities v_1 and v_2 are placed after the position of the dragon-king. The fifth component and the weight are, as follows

$$\langle v_1\, v_2\rangle_5(\Delta t) \stackrel{\text{def.}}{=} \frac{1}{t_R - \Delta t} \sum_{t'=t_{tot}-t_R+dt}^{t_{tot}-\Delta t} v(t')\, v(t'+\Delta t),$$
$$w_5 \stackrel{\text{def.}}{=} \frac{t_R - \Delta t}{t_{tot} - \Delta t} \tag{C.12}$$

being analogous to those of the first component and weight. More precisely, they are defined for the case where both velocities v_1 and v_2 are placed inside the time interval $[t_{tot} - t_R, t_{tot}]$ (without dragon-king) and velocity v_2 can be also counted at time t_{tot}.

Subsequently, we can calculate the estimator, which already includes the full influence of the sustained dragon-king:

$$\begin{aligned} C_d(\Delta t) &= \langle v_1 v_2\rangle(\Delta t) - \langle v_1\rangle\langle v_2\rangle \\ &= \frac{\gamma_L - \Delta t/t_{tot}}{1 - \Delta t/t_{tot}}\langle v_1 v_2\rangle_1(\Delta t) + \frac{\gamma_R - \Delta t/t_{tot}}{1 - \Delta t/t_{tot}}\langle v_1 v_2\rangle_5(\Delta t) \\ &\quad \frac{\Delta t/t_{tot}}{1 - \Delta t/t_{tot}}\left(\langle v\rangle_L + \langle v\rangle_R\right) v_d + \frac{\gamma_d - \Delta t/t_{tot}}{1 - \Delta t/t_{tot}} v_d^2 \\ &\quad - \frac{1}{(1 - \Delta t/t_{tot})^2}\left[\gamma_L\langle v\rangle_L + (\gamma_R - \Delta t/t_{tot})\langle v\rangle_R + \gamma_d v_d\right] \\ &\quad \times \left[(\gamma_L - \Delta t/t_{tot})\langle v\rangle_L + \gamma_R\langle v\rangle_R + \gamma_d v_d\right] \end{aligned} \tag{C.13}$$

by using definitions

$$\begin{aligned} \langle v_1\rangle &\stackrel{\text{def.}}{=} \frac{1}{t_{tot} - \Delta t}\left[\sum_{t'=dt}^{t_L} v(t') + \sum_{t'=t_{tot}-t_R+dt}^{t_{tot}-\Delta t} v(t')\right] + \frac{t_d\, v_d}{t_{tot} - \Delta t} \\ &= \frac{1}{t_{tot} - \Delta t}\left[t_L\langle v\rangle_L + (t_R - \Delta t)\langle v\rangle_R + t_d v_d\right], \\ \langle v_2\rangle &\stackrel{\text{def.}}{=} \frac{1}{t_{tot} - \Delta t}\left[\sum_{t'=\Delta t+dt}^{t_L} v(t') + \sum_{t'=t_{tot}-t_R+dt}^{t_{tot}} v(t')\right] + \frac{t_d\, v_d}{t_{tot} - \Delta t} \\ &= \frac{1}{t_{tot} - \Delta t}\left[(t_L - \Delta t)\langle v\rangle_L + t_R\langle v\rangle_R + t_d v_d\right], \end{aligned} \tag{C.14}$$

where $\langle v\rangle_L$ and $\langle v\rangle_R$ are the partial mean velocities of the random walk on the left and right sides of the dragon-king, respectively (cf. Fig. 1). We set velocities $\langle v_1\rangle_J$, $\langle v_2\rangle_J$, $J = L, R$, equal to zero as no drift is present in the system. Besides, we used dimensionless parameters $\gamma_L \stackrel{\text{def.}}{=} t_L/t_{tot}$, $\gamma_R \stackrel{\text{def.}}{=} t_R/t_{tot}$ and $\gamma_d \stackrel{\text{def.}}{=} t_d/t_{tot}$.

Because drift is absent in the system, Eq. (C.13), taking into account Definitions (C.14), assumes a simpler form

$$C_d(\Delta t) = \frac{\gamma_L - \Delta t/t_{tot}}{1-\Delta t/t_{tot}}\langle v_1 v_2\rangle_1(\Delta t) + \frac{\gamma_R - \Delta t/t_{tot}}{1-\Delta t/t_{tot}}\langle v_1 v_2\rangle_5(\Delta t) + \frac{v_d^2}{1-\Delta t/t_{tot}} \times \left[\gamma_d\left(1-\frac{\gamma_d}{1-\Delta t/t_{tot}}\right) - \frac{\Delta t}{t_{tot}}\right] = \frac{\gamma_L - \Delta t/t_{tot}}{1-\Delta t/t_{tot}}\, C_L(\Delta t) + \frac{\gamma_R - \Delta t/t_{tot}}{1-\Delta t/t_{tot}}\, C_R(\Delta t) + \frac{v_d^2}{1-\Delta t/t_{tot}}\left[\gamma_d\left(1-\frac{\gamma_d}{1-\Delta t/t_{tot}}\right) - \frac{\Delta t}{t_{tot}}\right], \tag{C.15}$$

where $C_L(\Delta t) = \langle v_1\, v_2\rangle_1(\Delta t)$ is an estimator of partial velocity autocorrelation function for time series present before dragon-king appearance while $C_R(\Delta t) = \langle v_1 v_2\rangle_5(\Delta t)$ after it.

As is apparent, the quantity $C_d(\Delta t)$ depends (in general) not only on the relative variable $\Delta t/t_{tot}$ but also on the parameters γ_L, γ_R, and γ_d. Hence, this quantity depends upon the position of the dragon-king inside a time series. That is, this quantity is, generally, non-stationary. However, it does not depend upon the sign of the dragon-king velocity. Moreover, the origin of the dragon-king is irrelevant. That is, our derived formula is sufficiently generic in the sense that it is valid not only for WM-CTRW but for any random walk.

For sufficiently wide time window Δt_{max}, which still obeys $\Delta t_{max}/t_{tot} \ll 1$, the quantity $C_d(\Delta t)$ simplifies to the asymptotic formula

$$C_d(\Delta t) \approx \frac{v_d^2}{1-\Delta t/t_{tot}}\left[\gamma_d\left(1-\frac{\gamma_d}{1-\Delta t/t_{tot}}\right) - \frac{\Delta t}{t_{tot}}\right]. \tag{C.16}$$

As long as the dragon-king is present, $C_d(\Delta t)$ does not vanish, even though estimators $\langle v_1\, v_2\rangle_1(\Delta t)$ and $\langle v_1\, v_2\rangle_5(\Delta t)$ (which can strongly fluctuate) are decaying.

Formula (C.16) takes a simpler form

$$C_d(\Delta t) \approx \gamma_d(1-\gamma_d)v_d^2 \tag{C.17}$$

if a strong but reasonable inequality

$$\frac{\Delta t_{max}}{t_{tot}} \ll min(\gamma_L,\, \gamma_R,\, \gamma_d\,(1-\gamma_d)) \tag{C.18}$$

holds.

C.2. $C_d(\Delta t)$ for the case of a shock (case (ii) of Sect. 2)

In order to consider the case of a shock within a time series, we replace Assumption (b), given in Sect. C.1, by the following one

$$t_d = dt. \tag{C.19}$$

That is, the duration of the dragon-king is assumed to be as short as possible and equal to the time discretization step dt. Assumption (C.19) imposes a modification of components $m = 2$ and $m = 4$ in Expression (C.7). Namely, components $m = 2$ and $m = 4$, together with their corresponding weights, are replaced by expressions

$$\langle v_1 v_2\rangle_2 \stackrel{\text{def.}}{=} v_L\, v_d, \qquad w_1 = \frac{dt}{t_{tot}-\Delta t}$$

and

$$\langle v_1 v_2 \rangle_4 \stackrel{\text{def.}}{=} v_d\, v_R, \qquad w_2 = \frac{dt}{t_{tot} - \Delta t},$$

respectively. Furthermore, instead of the component $m = 3$, we have

$$\langle v_1 v_2 \rangle_3, \qquad w_3 = \frac{\Delta t - dt}{t_{tot} - \Delta t},$$

where the current velocities $v_1 = v_L$ and $v_2 = v_R$ are now located before and after the position of the shock, respectively. Hence, the new relation for $C_d(\Delta t)$ is

$$\begin{aligned} C_d(\Delta t) = {} & \frac{t_L - \Delta t}{t_{tot} - \Delta t} \langle v_1 v_2 \rangle_1(\Delta t) + \frac{dt}{t_{tot} - \Delta t}\, v_L\, v_d + \frac{\Delta t - dt}{t_{tot} - \Delta t} \langle v_1\, v_2 \rangle_3(\Delta t) \\ & + \frac{dt}{t_{tot} - \Delta t}\, v_d\, v_R + \frac{t_R - \Delta t}{t_{tot} - \Delta t} \langle v_1 v_2 \rangle_5(\Delta t) - \frac{1}{(t_{tot} - \Delta t)^2} \left[t_L \langle v \rangle_L \right. \\ & \left. + dt\, v_d + (t_R - \Delta t) \langle v \rangle_R \right] \left[(t_L - \Delta t) \langle v \rangle_L + dt\, v_d + t_R \langle v \rangle_R \right] \\ = {} & \frac{t_L - \Delta t}{t_{tot} - \Delta t}\, C_L(\Delta t) + \frac{dt}{t_{tot} - \Delta t}\, v_L\, v_d + \frac{\Delta t - dt}{t_{tot} - \Delta t}\, C_{LR}(\Delta t) \\ & + \frac{dt}{t_{tot} - \Delta t}\, v_d\, v_R + \frac{t_R - \Delta t}{t_{tot} - \Delta t}\, C_R(\Delta t) \\ & - \frac{1}{(t_{tot} - \Delta t)^2} \left[t_L \langle v \rangle_L + dt\, v_d + (t_R - \Delta t) \langle v \rangle_R \right], \end{aligned} \tag{C.20}$$

where partial autocorrelation functions $C_L(\Delta t) = \langle v_1\, v_2 \rangle_1(\Delta t)$, $C_{LR}(\Delta t) = \langle v_1\, v_2 \rangle_3(\Delta t)$, and $C_R(\Delta t) = \langle v_1\, v_2 \rangle_5(\Delta t)$. Note that $C_{LR}(\Delta t)$ is the autocorrelation function for Δt enveloping the dragon-king.

Appendix D. Mean-square displacement vs. black swan

From Eqs. (24) and (25), we obtain

$$\begin{aligned} \frac{\overline{X^2}(L)}{(b_0)^2} & \approx N^{j_{max}} \frac{(b^2/N)^{j_{max}+1} - 1}{b^2/N - 1} \\ & \approx \begin{cases} \frac{1}{1 - N/b^2}\, (b^2)^{j_{max}}, & \text{for } b^2/N > 1 \\ \frac{1}{1 - b^2/N}\, N^{j_{max}}, & \text{for } b^2/N < 1 \end{cases} \end{aligned} \tag{D.1}$$

or equivalently

$$\frac{\overline{X^2}(L)}{(b_0)^2} \approx \begin{cases} \frac{(1-1/N)^{2/\beta}}{1 - 1/N^{2/\beta - 1}}\, L^{2/\beta}, & \text{for } \beta < 2 \\ \frac{1 - 1/N}{1 - b^2/N}\, L, & \text{for } \beta > 2 \end{cases} \tag{D.2}$$

as well as

$$\overline{X^2}(L) \approx \begin{cases} \frac{1}{1 - 1/N^{2/\beta - 1}}\, (x_{max})^2, & \text{for } \beta < 2 \\ (b_0)^2\, \frac{1 - 1/N}{1 - N^{2/\beta - 1}}\, L, & \text{for } \beta > 2 \end{cases} \tag{D.3}$$

where the number of steps

$$\begin{aligned} L & \approx N^{j_{max}} + N^{j_{max}-1} + N^{j_{max}-2} + \ldots + N^0 \\ & \approx \frac{1}{1 - 1/N}\, N^{j_{max}} \end{aligned} \tag{D.4}$$

and the single-step displacement of the black swan is defined by

$$x_{max} = b_0\, b^{j_{max}}. \tag{D.5}$$

Herein, the marginal case of $\beta = 2$ is not considered. As is apparent, for $\beta < 2$, i.e., if $\langle X^2 \rangle$ scales with L according to some power law, $\overline{X^2}$ is fully determined by x^2_{max} (cf. the first row in Expression (D.3)). This result is exactly what we need for illustration of our considerations. That is, the quantities (herein the mean-square displacement of the process) characterizing the system are mainly expressed by the corresponding quantities (herein, a single-step displacement) defining the black swans.

References

1. D. Sornette, *Critical Phenomena in Natural Sciences. Chaos, Fractals, Self-organization and Disorder: Concepts and Tools*, 2nd edn., *Springer Series in Synergetics* (Springer-Verlag, Heidelberg, 2004)
2. S. Albeverio, V. Jentsch, H. Kantz (eds.), *Extreme Events in Nature and Society* (Springer-Verlag, Berlin, 2006)
3. A. Bunde, Sh. Havlin (eds.), *Fractals and Disordered in Science*, Second Revised and Enlarged Edition (Springer-Verlag, Berlin, 1996)
4. A. Bunde, Sh. Havlin (eds.), *Fractals in Science* (Springer-Verlag, Berlin, 1995)
5. Sh. Havlin, D. ben-Avraham, Adv. Phys. **36**, 695 (1987)
6. D. ben-Avraham, Sh. Havlin, *Diffusion and Reactions in Fractals and Disordered Systems* (Cambridge University Press, Cambridge, 2000)
7. J.-P. Bouchaud, A. Georges, Phys. Rep. **195**, 127 (1990)
8. R. Metzler, J. Klafter, Phys. Rep. **339**, 1 (2000)
9. M. Shlesinger, G.M. Zaslavsky, U. Frisch (eds.), *Lévy Flights and Related Topics in Physics*, LNP 450 (Springer-Verlag, Berlin, 1995)
10. R. Kutner, A. Pękalski, K. Sznajd-Weron (eds.), *Anomalous Diffusion. From Basics to Applications* LNP **519** (Springer-Verlag, Berlin, 1999)
11. R.N. Mantegna, H.E. Stanley, *Econophysics. Correlations and Complexity in Finance* (Cambridge University Press, Cambridge, 2000)
12. Y. Malevergne, D. Sornette, *Extreme Financial Risks. From Dependence to Risk Management* (Springer-Verlag, Berlin, 2006)
13. D. Sornette, Int. J. Terraspace Eng. **2**, 1 (2009)
14. J. Laherrère, D. Sornette, EPJ B **2**, 525 (1999)
15. *Engineering Statistical Handbook*, National Institute of Standards and Technology (2007)
16. R. Kutner, Physica A **264**, 84 (1999)
17. R. Kutner, M. Regulski, Physica A **264**, 107 (1999)
18. R. Kutner, F. Świtała, Quant. Fin. **3**, 201 (2003)
19. R. Kutner, F. Świtała, EPJ B **33**, 495 (2003)
20. J.-P. Bouchaud, J. Phys. I (France) **2**, 1705 (1992)
21. H. Weissman, G.H. Weiss, Sh. Havlin, J. Stat. Phys. **57**, 301 (1989)
22. G.H. Weiss, *Aspects and Applications of the random Walk* (North Holland, Amsterdam, 1994)
23. G. Pfister, H. Scher, Adv. Phys. **27**, 747 (1978)
24. J. Haus, K.W. Kehr, Phys. Rep. **150**, 263 (1987)
25. M. Kozłowska, R. Kutner, Physica A **357**, 282 (2005)
26. M.S. Taqqu, V. Teverowsky, W. Willinger, Fractals **3**, 785 (1995)
27. G. Margolin, E. Barkai, Phys. Rev. Lett. **94**, 080601 (2005)
28. G. Bel, E. Barkai, Phys. Rev. Lett. **94**, 240602 (2005)
29. G. Bel, E. Barkai, Phys. Rev. E **73**, 016125 (2006)
30. D. Sornette, *Probability Distributions in Complex Systems*, core article for *Encyclopedia of Complexity and Systems Science*, edited by R.A. Meyers (Springer-Varlag, Berlin, 2009)